Burner Tubing Specification for the Turbulent Ethylene Non-Premixed Jet Flame

Figure 1 shows a schematic of the burner used to support the turbulent ethylene non-premixed jet flames. The dimensions of the two co-annular tubes in the burner are given below. Note that the tubing for both tubes is smooth-bore seamless type 304 stainless steel, straight cut at the end. The perforated plate that supports the pilot flames was carefully designed in an attempt to provide a uniform exit flow rate across the pilot flame annulus and is recessed 3.2 mm from the burner face. A detailed description of the pilot design is given by Zhang et al. [1]. The burner is surrounded by a well-conditioned coflow of dry air with a velocity of 0.6 m/s.

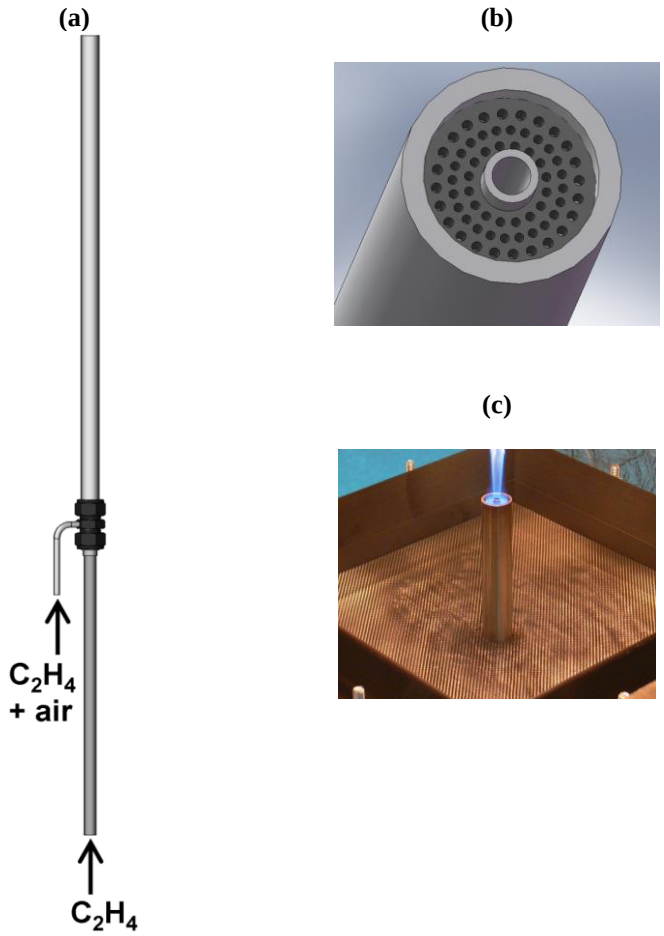

Figure 1. The piloted jet burner: (a) drawing of the burner, with the central fuel tube supplying the fuel and the outer coannular tube supplying a premixed fuel-air mixture to an array of small pilot flames; (b) close-up view of the burner exit, showing the fuel tube surrounded by a perforated pilot plate; (c) base of a burning ethylene flame, with pilot flames appearing as small blue cones surrounding the main jet.

Fuel Tube:
OD 4.78 mm ID 3.35 mm

Co-annular Tube (surrounding the flame pilot):
OD 19.05 mm ID 14.83 mm

The length of the fuel tube (unobstructed) is 540 mm (161 jet diameters) which should assure a fully developed turbulent flow profile exiting the pipe.

References

[1] J. Zhang, C.R. Shaddix, R.W. Schefer, Rev. Sci. Instr.82 (2011) 074101.

Spatially Resolved Measurements of Radiant Emission from Turbulent Ethylene Non-Premixed Jet Flames

Figure 1 shows the schematic of the radiation experiments. The radiometer is a thin-film based thermopile detector (Dexter, Type 1M), and its calcium fluoride window transmits flame emission of wavelength between 0.2 and 8 μm, which covers almost all the important radiation bands in flames. A black-anodized, water-cooled steel tube restricts incident radiation within a small solid angle (Ω) of 1.065 x 10^{-4} sr. The detector sensor is located 500 mm away from the jet axis. Therefore, the radiometer measures the incident radiation that is emitted within a cone with a base diameter of **5.8 mm** at the flame axis.

During experiments, the burner is traversed axially or radially to measure radiation along different paths (Fig. 1). As the radiative heat exchange and the electronic response of the thermopile detector are affected by its own temperature, great care has been taken to stabilize the thermal environment of the detector, such as covering the detector case with aluminum foil to shield flame radiative heating. In addition, three thermocouples are attached to the detector case to monitor its temperature, which is used to correct for the effects due to detector temperature rise as described below.

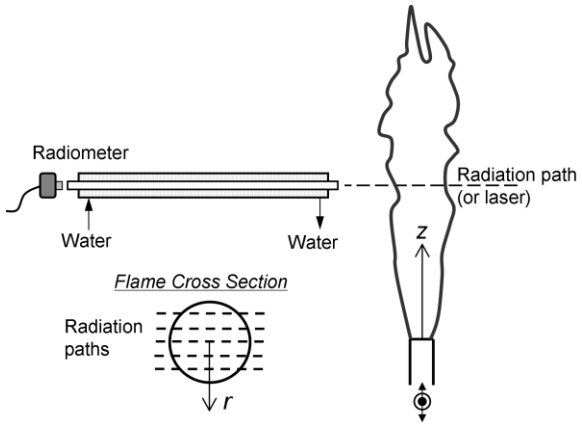

Figure 1. Schematic of radiation experiments (not to scale). A water-cooled housing surrounds the black anodized sight tube that extends from the detector face. The dashed line designates the radiation path. The radiometer is located 500 mm away from the jet axis.

For an ideal thermopile detector, the signal output is expressed as (Dexter Research Center),

$$S = \Re \phi A_d , \qquad (1)$$

with $\Re$ being the linear responsivity of the detector (incorporating the subsequent amplification gain), ϕ the net radiative flux received by the detector, and A_d the detector active area. As shown by Incropera and DeWitt [1], a radiation heat transfer analysis yields

$$\phi = G_F'' - \varepsilon_d \sigma \left(T_d^{\,4} - T_w^{\,4} \right), \qquad (2)$$

where G_F'' is the measured incident radiation flux from the flame, ε_d is the emissivity of the detector, σ is the Stefan-Boltzmann constant, and T_d and T_w are the temperature of the detector and the sight tube wall, respectively (Fig. 1). Deduction of Eq. (2) assumes a uniform temperature of T_w for the sight tube, which is deemed reasonable with our

temperature-controlled water cooling. As G_F'' is the collected flame radiation falling within the solid angle Ω, we may further define a quantity independent of the sight tube geometry as

$$I = G_F'' / \Omega, \qquad (3)$$

which is termed as the total-spectrum radiant intensity. Combination of Eqs. (1-3) gives rise to,

$$S = \Re A_d \Omega \cdot I + \Re A_d \varepsilon_d \sigma \left(T_d^{\,4} - T_w^{\,4} \right) = C_1 I + C_2 \left(T_d^{\,4} - T_w^{\,4} \right), \qquad (4)$$

with $C_1 = \Re A_d \Omega$, and $C_2 = \Re A_d \varepsilon_d \sigma$, which can be determined though calibration using a black-body radiation source at various temperatures, which we performed, as shown in Fig. 2.

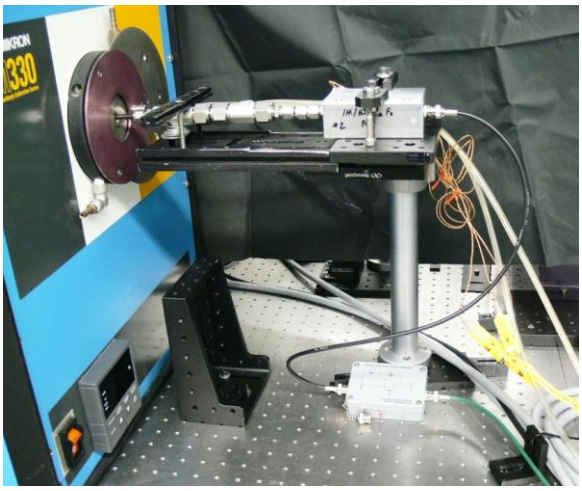

Figure 2. Photograph of radiometer being calibrated with a high temperature blackbody source.

Because of the intrinsic thermal inertia, the thermopile detector has a finite time constant τ of 12.8 ms. Measurement of fluctuating radiative intensity with this detector is equivalent to applying a low-frequency-pass filter, with the 3dB cut-off frequency as:

$$f_{3dB} = 1/(2\pi\tau) = 12.4\ Hz\,. \qquad (5)$$

The implications are that this detector is unable to keep up with high-frequency fluctuating radiation. As a result, this thermopile detector can accurately measure the time-averaged radiant intensity, but would underestimate the root-mean-square (rms). Besides the bias resulting from frequency response, the uncertainties in radiation measurements result primarily from the electronic noise and the detector temperature offset, which amount to less than 3% uncertainty at most locations.

References

[1] Incropera, F. P. and D. P. DeWitt (1990). Fundamentals of Heat and Mass Transfer. New York, John Wiley & Sons.

Measurements of Soot Temperature in Turbulent Ethylene Non-Premixed Jet Flames

Figure 1 shows a schematic of the '3-line' soot diagnostic that was implemented. Laser attenuation was performed with a 632.8 nm HeNe laser, so that soot dimensionless extinction coefficients previously measured at this wavelength could be utilized to interpret the measurement. A reference laser intensity measurement was made using a beamsplitter and a photodiode detector with a 632.8 nm laser line filter (3 nm FWHM). After passing through the flame probe volume, the laser beam was separated from the 2-color soot emission signals with the use of a dichroic beamsplitter. The transmitted beam was collected in a 12-inch (30.5-cm) diameter integrating sphere, before passing through a laser line filter onto a photodiode detector, in order to remove any influence from turbulent flame beam steering on the attenuation measurement.

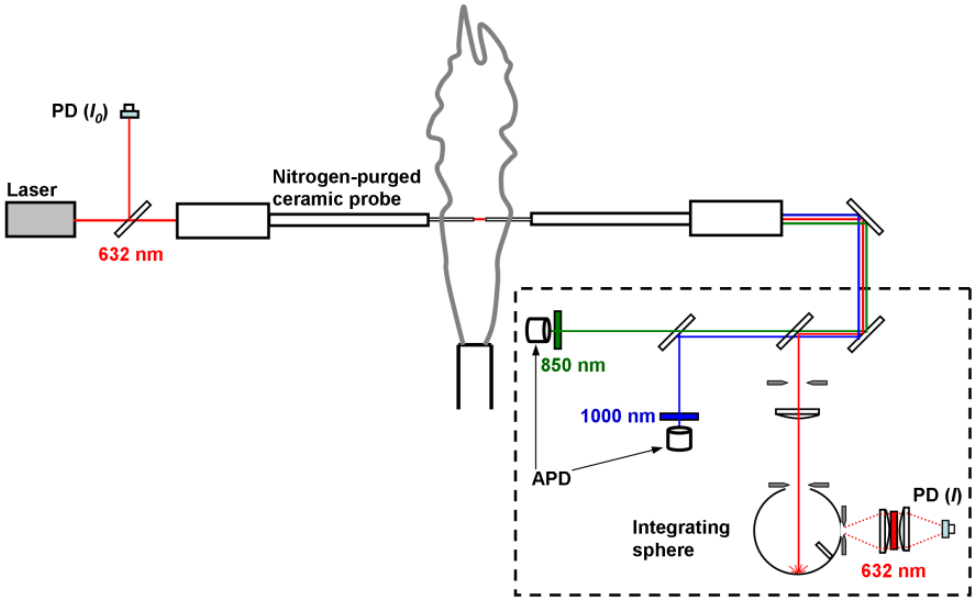

Figure 1. Schematic of diagnostic configuration used to perform 3-line measurements of soot

The soot emission signals were split with a cube beamsplitter and then passed through bandpass filters with center wavelengths of 850 nm and 1000 nm before passing onto thermoelectrically cooled silicon avalanche photodiode (APD) detectors. Calibration of the two-color pyrometry diagnostic was performed using a high-temperature blackbody source with a mirror that redirected the blackbody light to the avalanche photodiode detectors.

A key aspect of the 3-line diagnostic technique is the need to insert a two-ended probe into the flame to limit the length of the optical interrogation region. In previous studies, these probes have typically been constructed of water-cooled steel or aluminum tubing, in some cases with insulation wrapped around the outside of the probes. With this design approach, the probe tubes are necessarily quite large and also provide a thick thermal quench layer. To minimize probe perturbation of the flow field and flame sheets, we adopted the approach first used by Sivathanu and Faeth [1], with tapered, or, in our case, step-reduced, refractory probe ends that are uncooled. Figure 2 shows photographs of the cooled housings containing the outer probe ends and the uncooled probe tips that enter the flame. These probe tips have an OD of 0.25 in. (6.35 mm) and an ID of 0.175 in. (4.45 mm). A small flow of nitrogen (< 1 slpm) was introduced into each probe end to reduce the likelihood of soot deposition within the tubes.

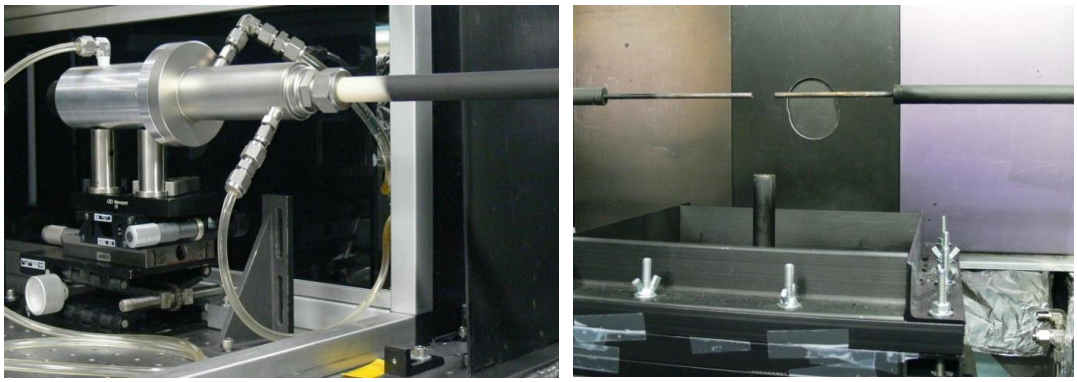

Figure 2. Optical probe for performing 3-line measurements of soot temperature/ concentration statistics in the turbulent jet flame. Aluminum optical housing (left) is water-cooled and provides N_2 purge gas. Refractory probe ends (right) are uncooled.

Early testing of the alumina probes revealed that they transmitted radiant emission from the broader flame through the probe walls to the pyrometry detectors at measurable levels. Therefore, the outer surfaces of the probes were painted black with high-temperature paint, which corrected this problem. In addition, a small amount of radiation was transmitted to the detectors from the hot tips of the probes when they were located in the hottest regions of the flames, leading to a non-zero radiant background signal. This background signal, which showed up as a baseline shift on the time records, was subtracted before processing the datasets to determine the soot radiant temperature.

Data collection and processing

Data were collected along the flame centerline at many different heights and radial traverses were performed at selected heights. A data sampling rate of 5 kHz was used to resolve the turbulent motion of the soot. Digital time records were collected as 40 sets of 5000 data points (i.e. a 1 sec time record) at a given location in the flame before a computer-controlled X-Y-Z translation stage moved the flame to the next programmed sampling position. A 10 mm probe end separation was used for most of the measurements, but some data were also collected for probe separations of 5 mm and 20 mm. The soot extinction measurement was converted to soot volume fraction according to the Beer-Lambert law with a dimensionless extinction coefficient, K_e, of 9.3, as determined in laminar flames by Williams et al. [2]. The optical path length of soot extinction was assumed to be equal to 2 mm less than the probe tip separation, to account for the effect of the small purge flow out the tips of the probe.

Measurement uncertainty

As previously demonstrated, the predominant source of uncertainty in measurements of soot volume fraction and soot temperature using the 3-line technique is due to uncertainties in the optical properties of soot [20]. Uncertainty in the dimensionless extinction coefficient at 632.8 nm dominates the uncertainty in the derived soot volume fraction, while uncertainty in the spectral variation of the absorptivity between 850 nm and 1000 nm (assumed here to follow a $1/\lambda$ dependence between these two wavelengths) dominates the uncertainty in the derived soot temperature. Based on our previously reported analysis [3], the uncertainty in soot volume fraction is estimated as ± 12%, in those regions where there is measurable laser beam attenuation, and the uncertainty in soot temperature is estimated as ± 3%.

In addition to these ‘static’ measures of experimental uncertainty with the 3-line diagnostic, in a turbulent flame there are additional uncertainties associated with variations in soot temperature across the optical probe volume [4], as well as variations in the soot optical properties in space and time in the flame. These additional uncertainties will increase the uncertainty in results derived from a given temporal record, but should have a minor influence on the uncertainty in the average data collected from the flame, except in locations where soot is undergoing active inception, where its optical properties are rapidly evolving.

References

[1] Y.R. Sivathanu, G.M. Faeth, Combust. Flame 81 (1990) 150-165.

[2] T.C. Williams, C.R. Shaddix, K.A. Jensen, and J.M. Suo-Anttila, Int. J. Heat and Mass Transfer 50 (2007) 1616-1630.
[3] J.J. Murphy, C.R. Shaddix, Combust. Sci. Technol. 178 (2006) 865-894.
[4] J.J. Murphy, C.R. Shaddix, Combust. Flame 143 (2005) 1–10.